Electronic Supplementary Information for

Facile preparation of hierarchically porous carbons from metal-organic gels and their application in energy storage

Wei Xia, Bin Qiu, Dingguo Xia & Ruqiang Zou*

* rzou@pku.edu.cn

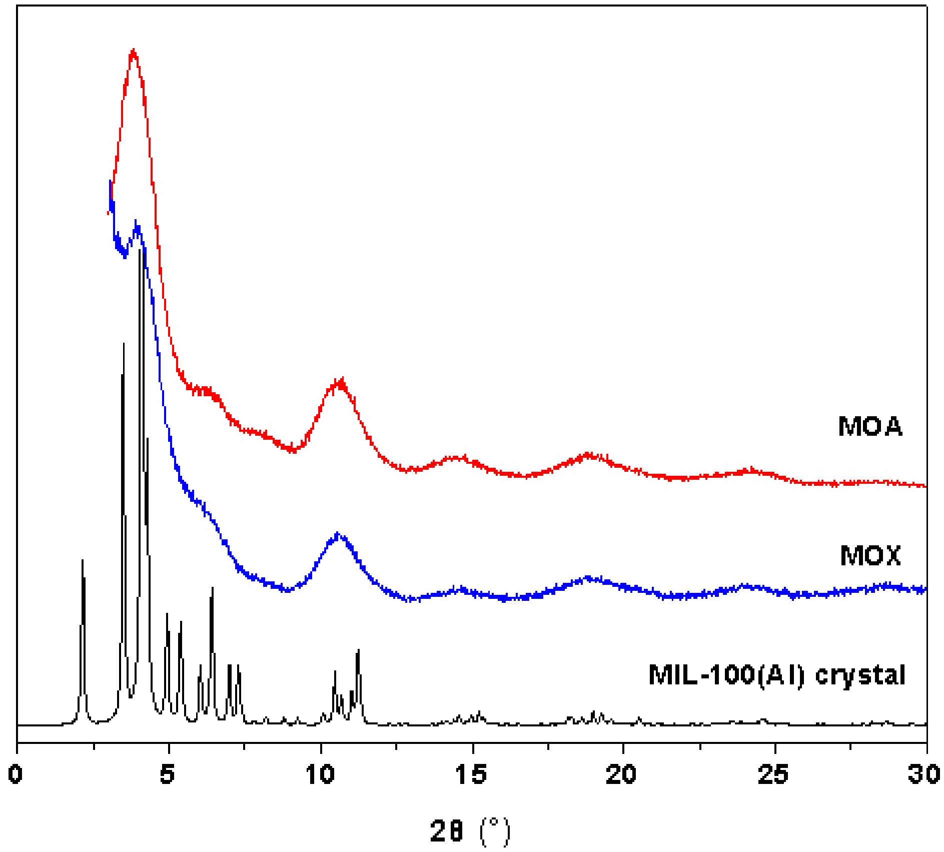

Figure S1. PXRD patterns of MOA, MOX and the simulated one from crystallographic information file of the MIL-100(Al) crystal.

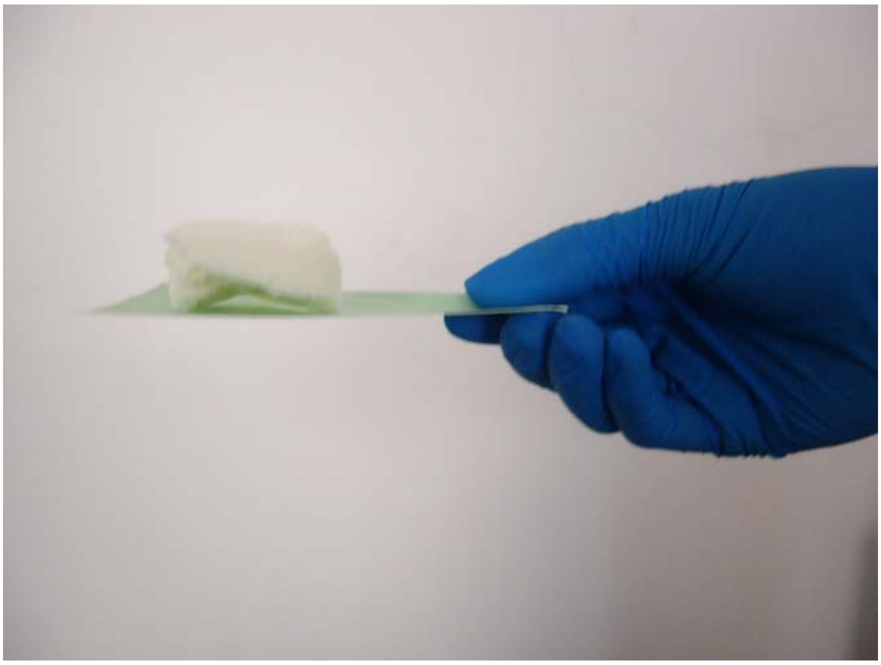

Figure S2. Photograph of a super light MOA monolith standing on a piece of note paper.

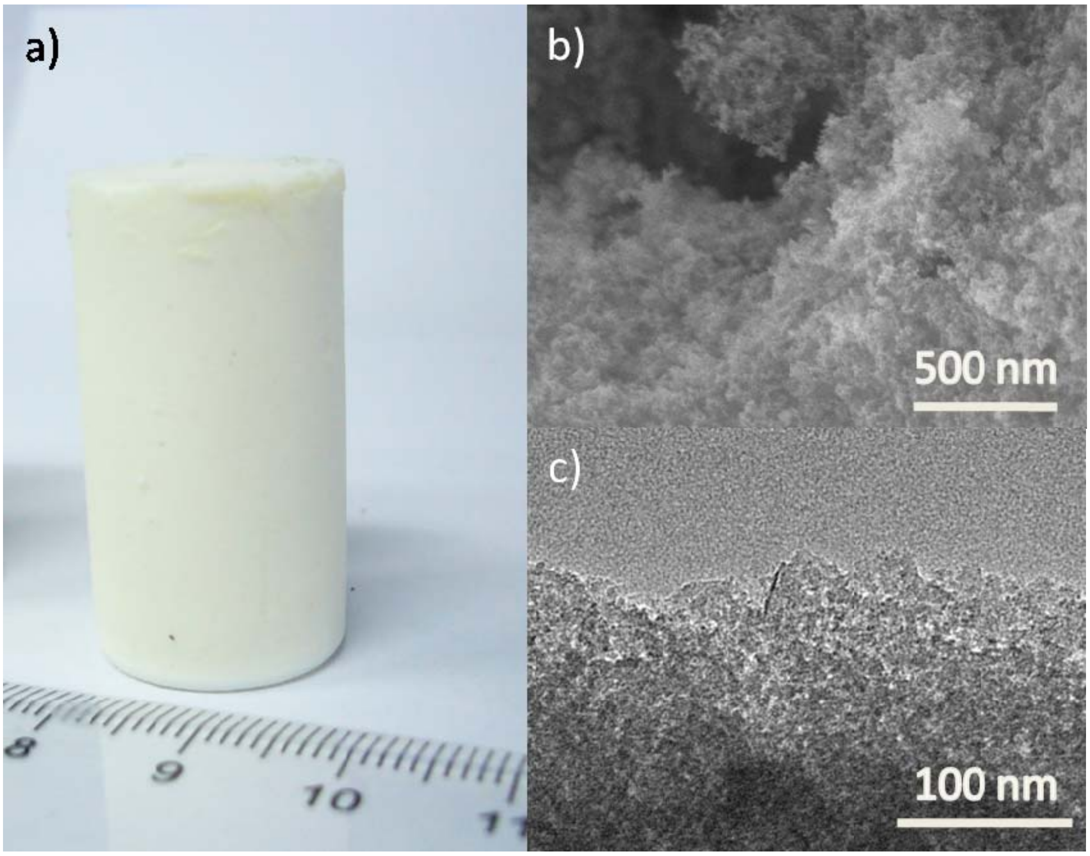

Figure S3. Images of the MOA: (a) Digital photograph, (b) SEM and c) TEM.

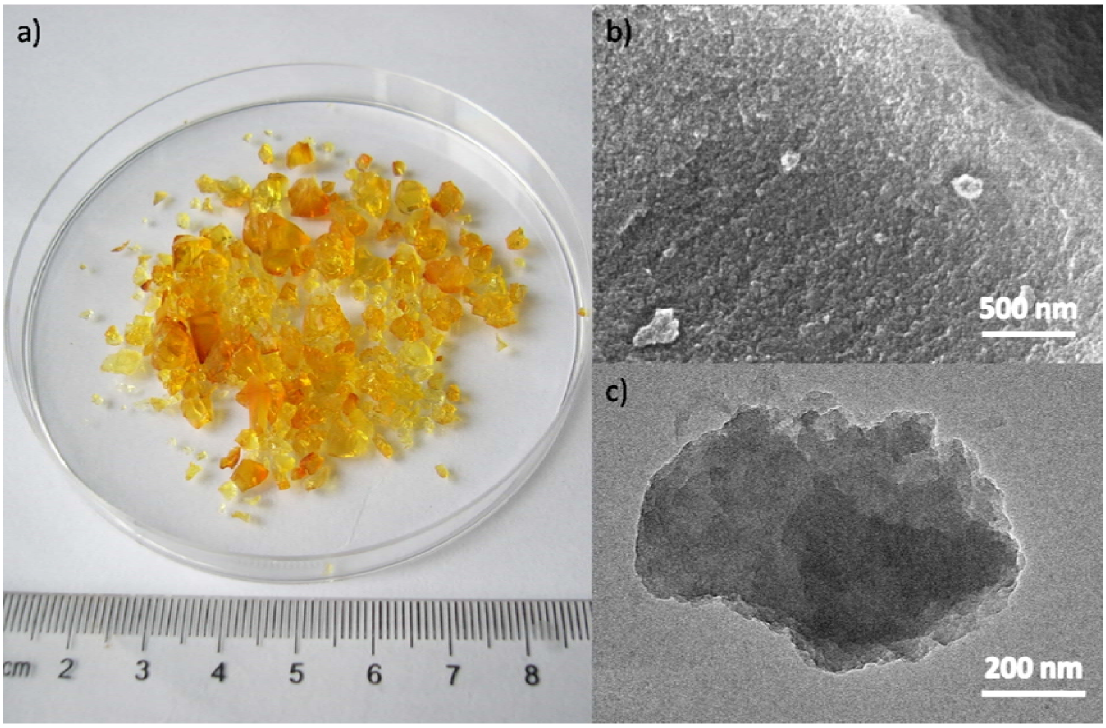

Figure S4. View of MOX samples: (a) Digital photograph, (b) SEM and (c) TEM.

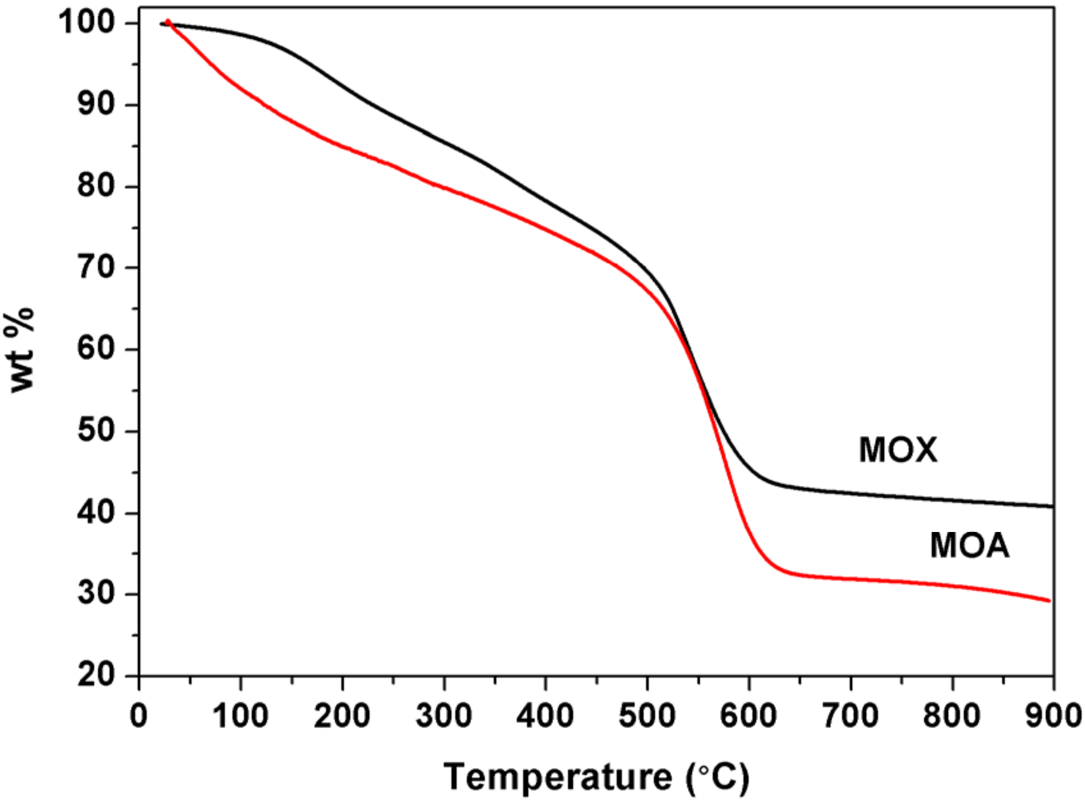

Figure S5. TGA curves of MOX and MOA.

Table S1 Elemental analysis of the carbon products.

Sample	C (wt %)	H (wt %)	N (wt %)	O (wt %)
MOX-C	93.4	0.8	0.4	5.4
MOA-C	91.3	2.1	0.5	6.1

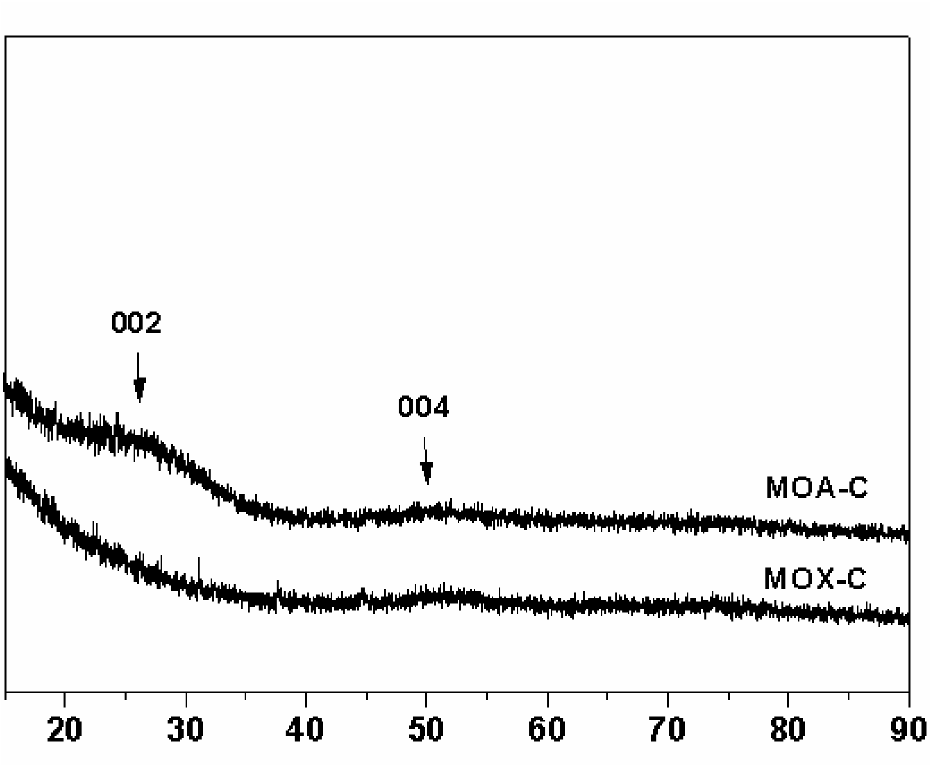

Figure S6. PXRD patterns of the MOX-C and MOA-C.

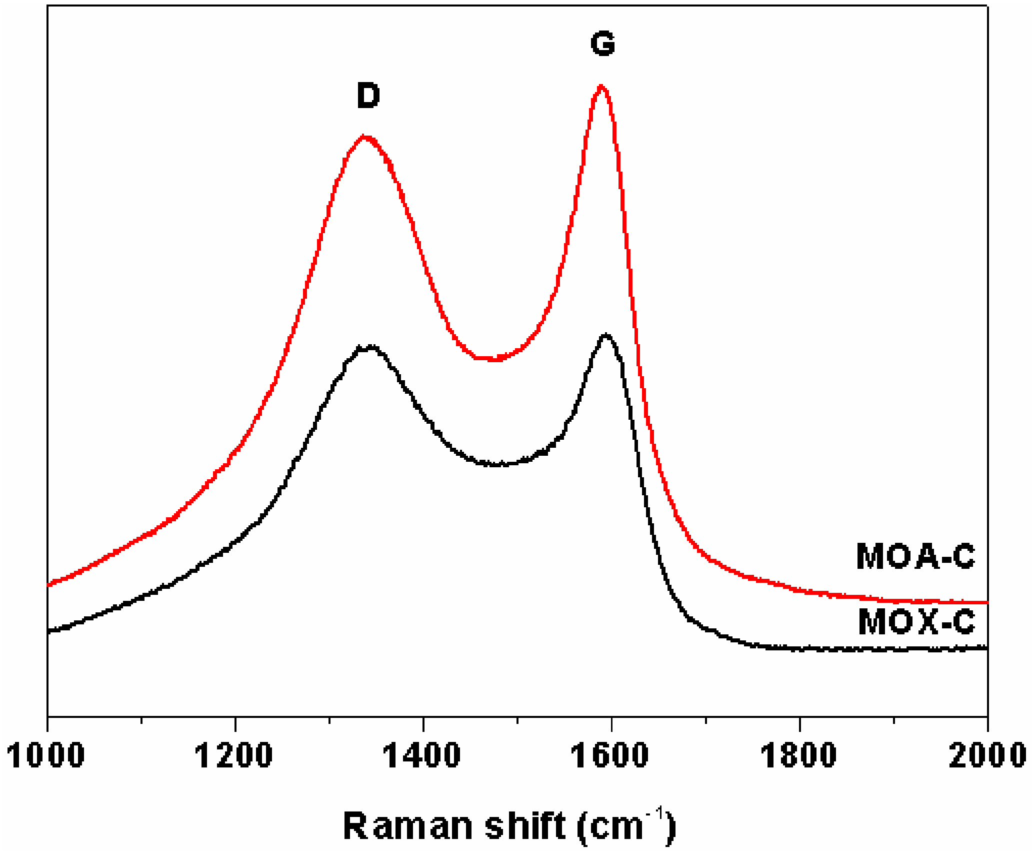

Figure S7. Raman spectra of MOX-C and MOA-C.

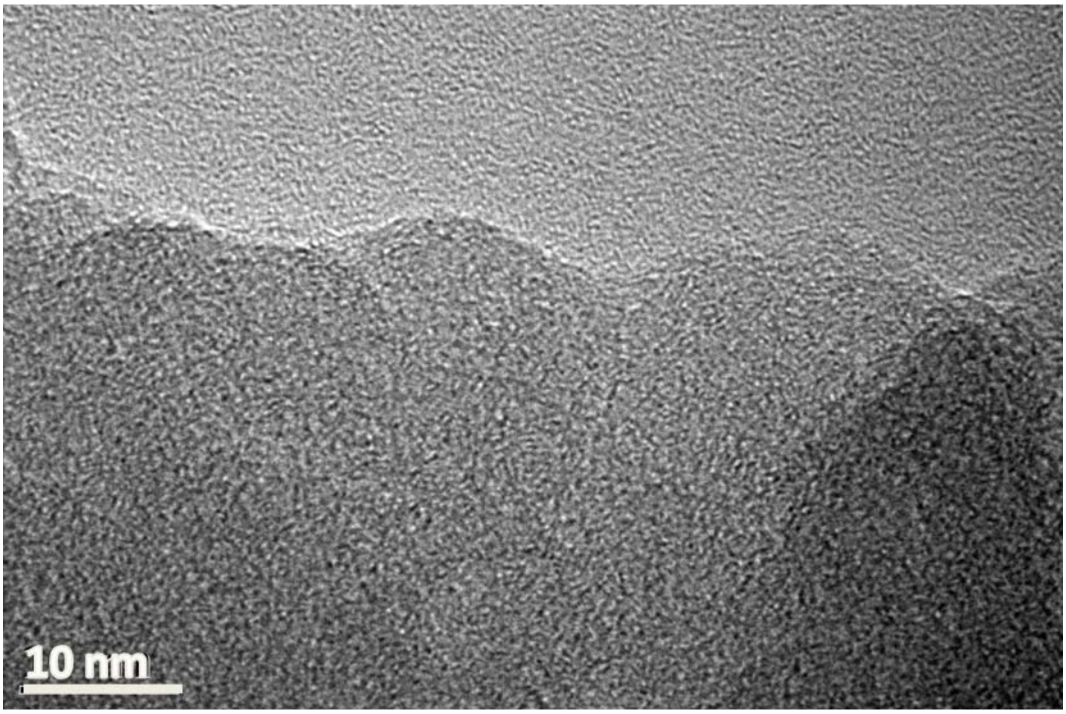

Figure S8. TEM image of MOX-C.

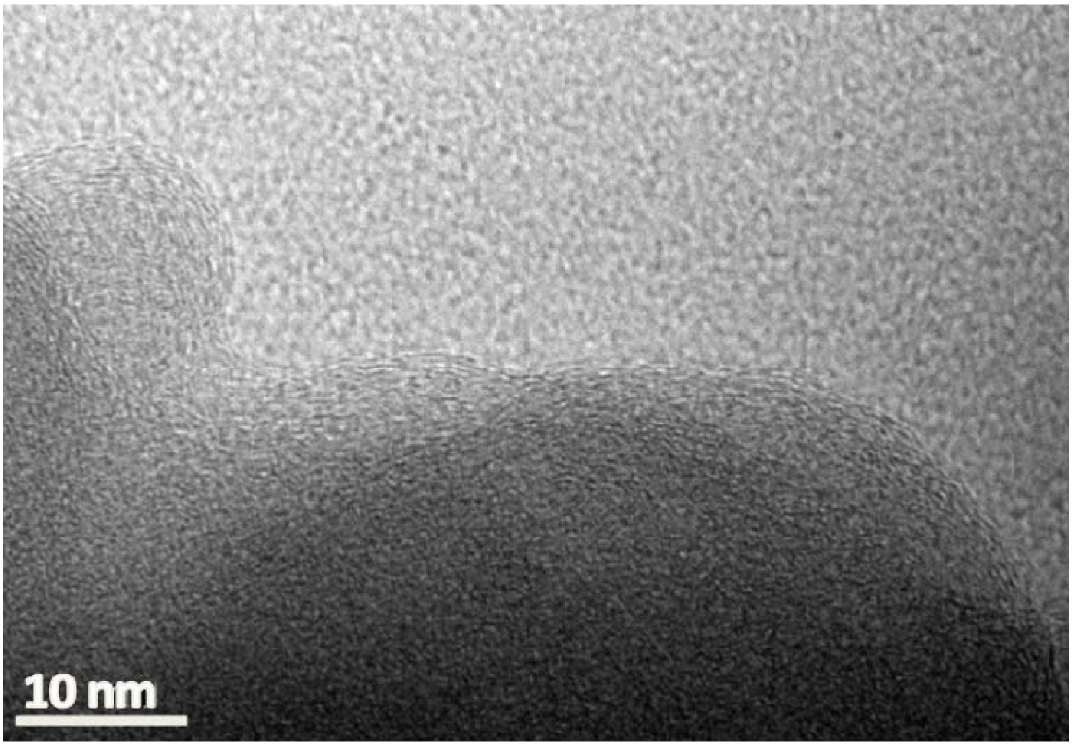

Figure S9. TEM image of MOA-C.

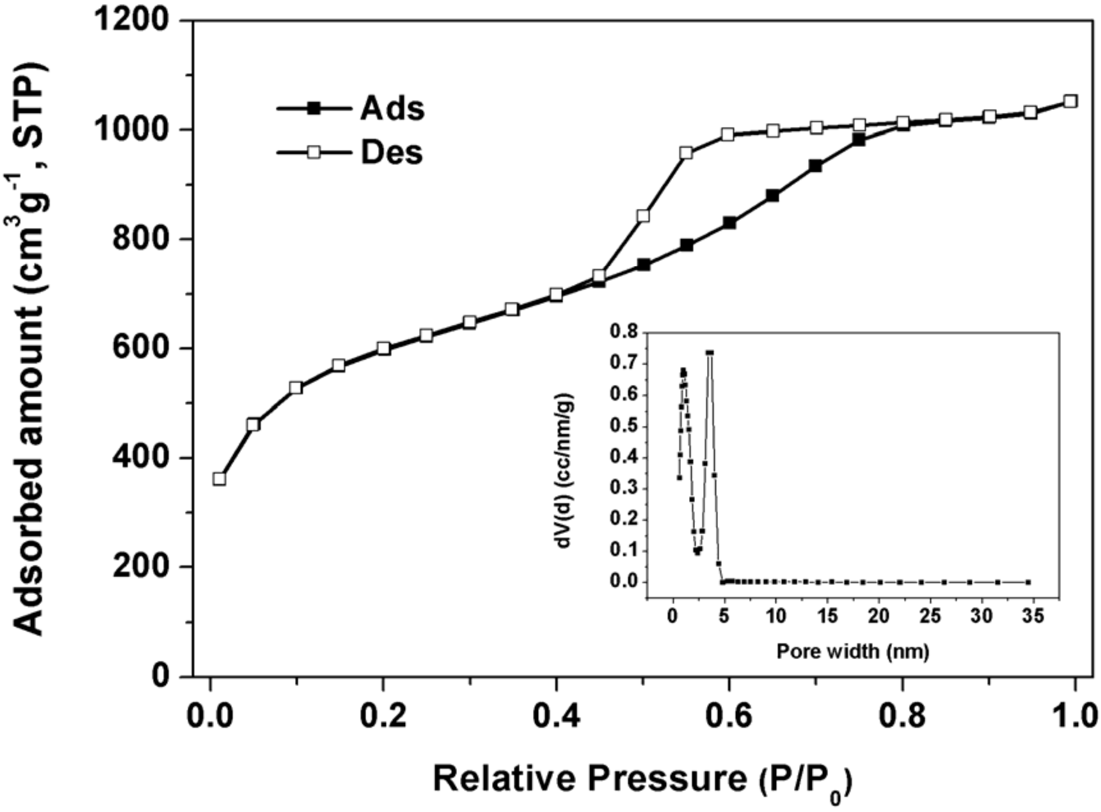

Figure S10. N_2 sorption isotherms at 77K and pore size distributions (inset) based on the QSDFT model of MOX derived carbon before KOH treatment. The BET surface area and pore volume are 2131 m^2g^{-1} and 1.63 cm^3g^{-1}, respectively.

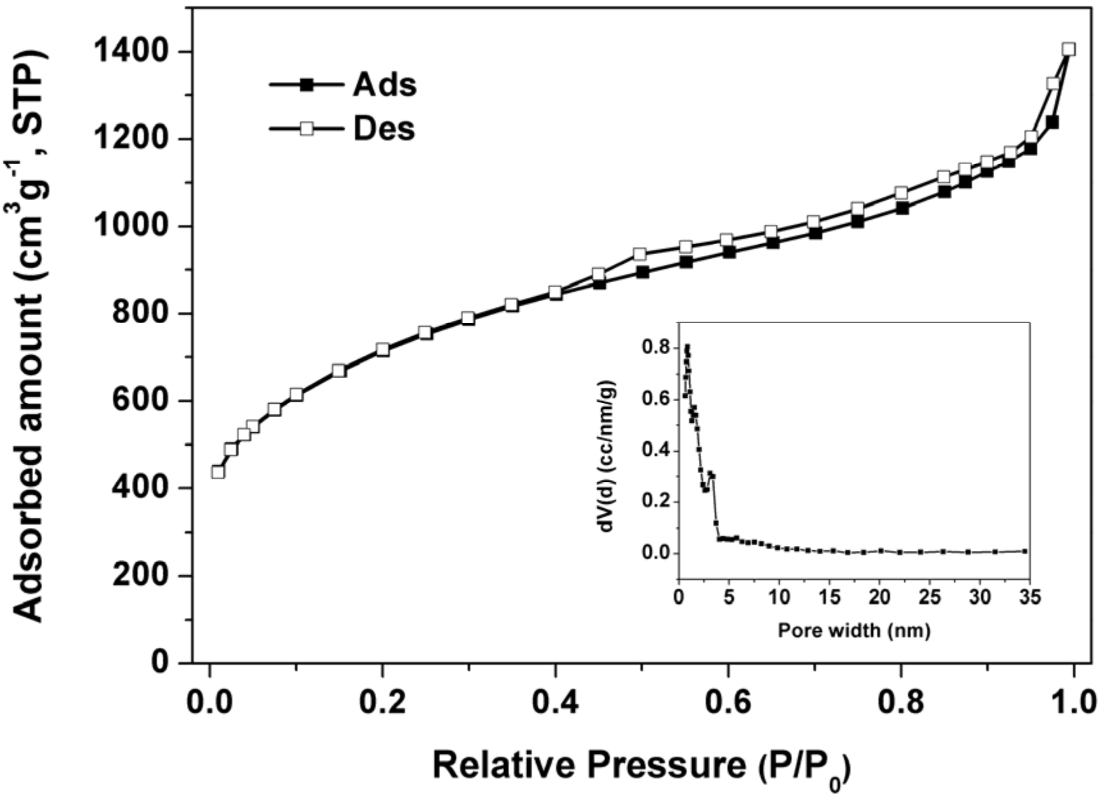

Figure S11. N_2 sorption isotherms at 77K and pore size distributions (inset) based on the QSDFT model of KOH treated MOA-C sample. The BET surface area and pore volume are 2523 m^2g^{-1} and 2.17 cm^3g^{-1}, respectively. After KOH activation, the BET surface area of the sample was enhanced (1820 m^2g^{-1} for MOA-C). However, the pore volume dramatically dropped down (3.22 cm^3g^{-1} for MOA-C) due to the collapse of the macropores.

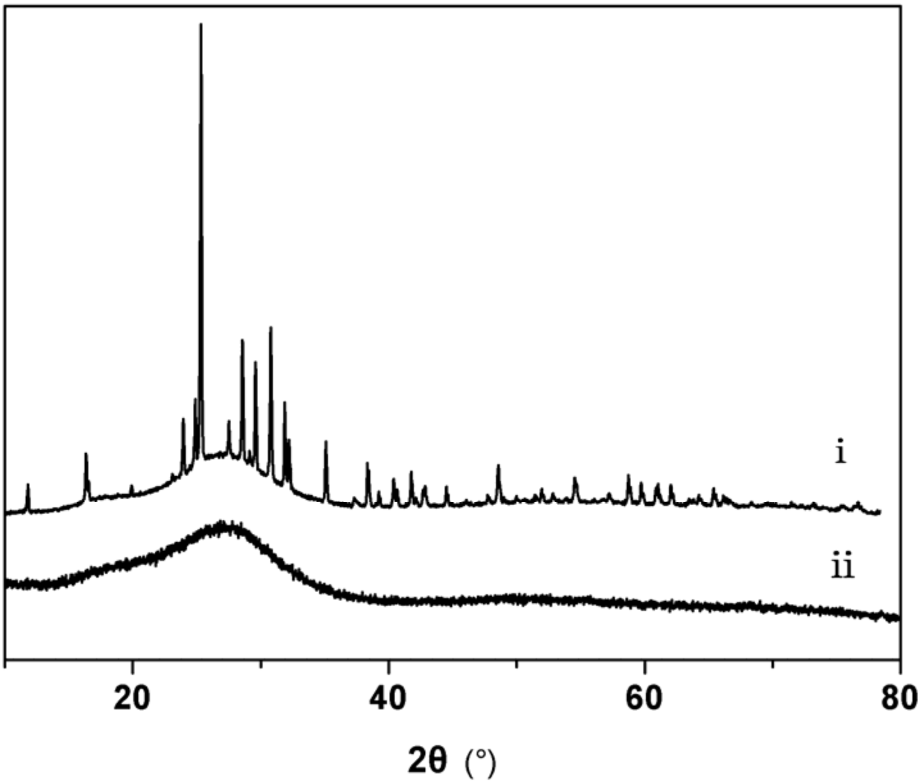

Figure S12. PXRD patterns of a mixture of MOA-C and sulfur (i) before heating and (ii) after heating at 300 °C.

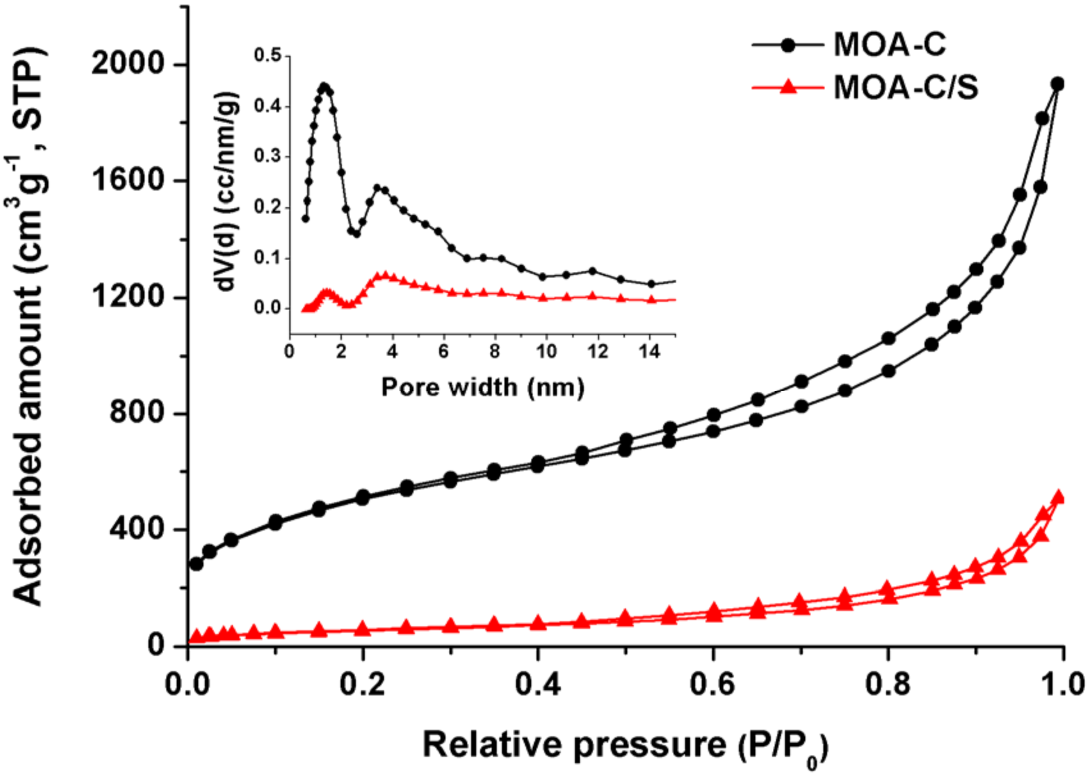

Figure S13. N_2 sorption isotherms at 77K and pore size distributions (inset) based on the QSDFT model of MOA-C before and after sulfur impregnation.

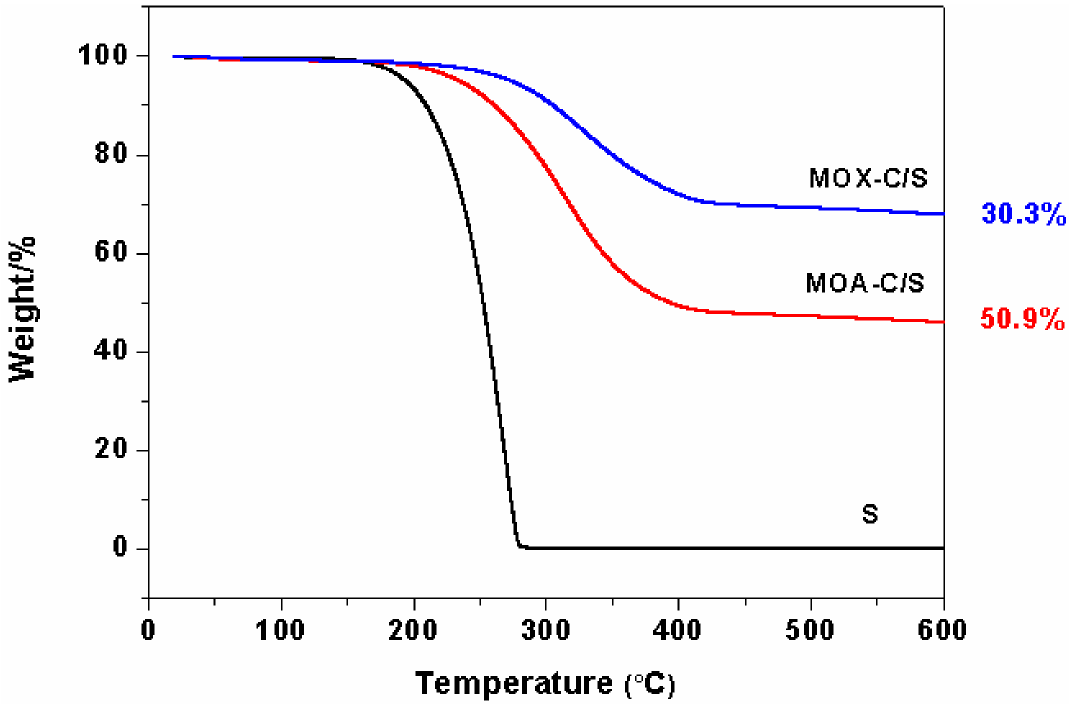

Figure S14. TGA curves of bare sulfur, MOX-C/S and MOA-C/S composites.